PROCEEDINGS A

rspa.royalsocietypublishing.org

Research

Cite this article: Mancarella F, Style RW, Wettlaufer JS. 2016 Surface tension and the Mori–Tanaka theory of non-dilute soft composite solids. *Proc. R. Soc. A* **472**: 20150853. http://dx.doi.org/10.1098/rspa.2015.0853

Received: 18 December 2015
Accepted: 8 April 2016

Subject Areas:
materials science, applied mathematics, mathematical modelling

Keywords:
surface tension, soft composites, elastic moduli

Author for correspondence:
John S. Wettlaufer
e-mail: john.wettlaufer@yale.edu

Surface tension and the Mori–Tanaka theory of non-dilute soft composite solids

Francesco Mancarella[1], Robert W. Style[2] and John S. Wettlaufer[1,2,3]

[1]Nordic Institute for Theoretical Physics (NORDITA), 10691 Stockholm, Sweden
[2]Mathematical Institute, University of Oxford, Oxford OX2 6GG, UK
[3]Yale University, New Haven, CT 06520, USA

JSW, 0000-0002-1676-9645

Eshelby's theory is the foundation of composite mechanics, allowing calculation of the effective elastic moduli of composites from a knowledge of their microstructure. However, it ignores interfacial stress and only applies to very dilute composites—i.e. where any inclusions are widely spaced apart. Here, within the framework of the Mori–Tanaka multiphase approximation scheme, we extend Eshelby's theory to treat a composite with interfacial stress in the non-dilute limit. In particular, we calculate the elastic moduli of composites comprised of a compliant, elastic solid hosting a non-dilute distribution of identical liquid droplets. The composite stiffness depends strongly on the ratio of the droplet size, R, to an elastocapillary lengthscale, L. Interfacial tension substantially impacts the effective elastic moduli of the composite when $R/L \lesssim 100$. When $R < 3L/2$ ($R = 3L/2$) liquid inclusions stiffen (cloak the far-field signature of) the solid.

1. Introduction

In a seminal paper, Eshelby described the strain response of isolated inclusions to applied stresses, and predicted the stiffness of solid composites containing a low volume fraction of inclusions [1]. These results have since been successfully used to model a huge range of problems, from composite mechanics to fracture and dislocation theory. As Eshelby's theory strictly only

THE ROYAL SOCIETY PUBLISHING

applies to composites containing dilute inclusions, it has been extended to treat non-dilute composites with a variety of approximation schemes [2–6], many of which show good agreement with experimental data across an unexpectedly wide range of inclusion volume fraction ϕ.

Although Eshelby's theory and its non-dilute extensions work well for hard composites, recent work has shown that they can fail to describe soft composites [7,8]. This is because such schemes view the constituents of the composite as bulk linear-elastic solids, while ignoring the physics of the interface between them [1–4,9,10]. However, as is generally the case in interfacial thermodynamics [11], when the inclusions become sufficiently small that the surface energy becomes appreciable relative to the bulk strain energy, one cannot ignore interfacial effects. For example, when the interface between an inclusion and the host (with Young's modulus E) is governed by an isotropic, strain-independent surface tension γ, the validity of the standard framework (e.g. [1–4,9,10]) is limited to inclusions much larger than the elastocapillary length $L \equiv \gamma/E$ [7,8]. Because in soft materials such as gels and elastomers (e.g. [12–15]), the interface between an inclusion and the host is typically governed by an isotropic, strain-independent surface tension γ and the inclusions can be large or small relative to L, what follows is of direct relevance to these and many other composite materials.

Here we extend Eshelby's theory to soft, non-dilute composites with an isotropic, strain-independent interfacial surface tension. In particular, motivated by recent experiments and their analysis [7,8], we focus on the problem of a soft elastic solid containing a non-dilute distribution of identical liquid droplets. The framework for our extension is the multiphase scheme introduced by Mori & Tanaka [9], and our approach generalizes previous theoretical results that have been compared with experiments on soft-aerated composites [16–18]. Our work differs from previous approaches that either consider dilute inclusions or interfacial elasticity (e.g. [7,19–21]), or that obtain upper and lower bounds on composite elastic moduli with interfacial elasticity [22–24].

2. The Mori–Tanaka, or Equivalent Inclusion-Average Stress, method

The concept of an equivalent inclusion [1] and the average stress in the matrix are central to the Mori–Tanaka approximation scheme, which we refer to as Equivalent Inclusion-Average Stress (EIAS) method (e.g. [25]). Here, we envision a two-phase system of inclusions in a host matrix. The inclusion phase consists of identical incompressible droplets randomly arranged in the solid elastic host matrix, as shown in figure 1. Under stress-free circumstances, the droplets are spherical.

Benveniste [25] described the central assumption of the EIAS method as being equivalent to requiring that the fourth-order tensor relating the average strain in a typical inclusion to the average strain in the matrix is equivalent to 'Wu's tensor', T_{ijkl}' [26]. Wu's tensor relates the uniform strain in an inclusion embedded in an 'all-matrix' material to the imposed uniform strain at infinity. Here, the inclusion phase is denoted with the superscript *, and the matrix phase is free of indices. Across the interface between the phases in the equivalent inclusion system, the stress and displacement are continuous (also known as perfect bonding conditions).

For a composite consisting of spherical elastic inclusions with bulk/shear moduli K^*, μ^* embedded in a matrix with moduli K, μ, the EIAS method gives that the effective composite moduli $\bar{K}, \bar{\mu}$ are (see eqns (31) and (32) of [25]):

$$\bar{K} = K + \phi(K^* - K)A_m \quad \text{and} \quad \bar{\mu} = \mu + \phi(\mu^* - \mu)A_s, \tag{2.1}$$

where

$$A_m = \frac{K}{K + (1-\phi)(K^* - K)S_m}, \quad A_s = \frac{\mu}{\mu + (1-\phi)(\mu^* - \mu)S_s},$$
$$S_m = \frac{1+\nu}{3(1-\nu)} \quad \text{and} \quad S_s = \frac{8-10\nu}{15(1-\nu)} \tag{2.2}$$

and ν is Poisson's ratio of the matrix.

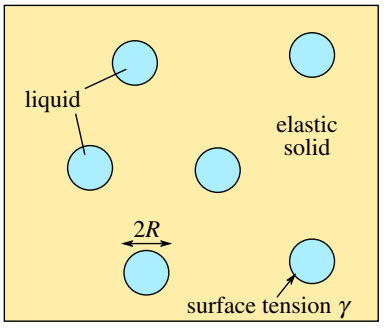

Figure 1. Schematic of the composite material treated. Identical liquid inclusion droplets are embedded in a solid elastic matrix. (Online version in colour.)

Here, we first show the equivalence between a droplet embedded in an elastic solid with an isotropic interfacial tension γ and a corresponding elastic inclusion with no interfacial tension. This allows us to calculate the moduli K^* and μ^*, which we can then substitute into the above equations to yield the effective composite properties.

3. Calculating the equivalent inclusion moduli

Following Style *et al.* [7,8], we model the boundary condition for the elastic stress at the surface of the droplet using the Young–Laplace equation for the discontinuity of the traction vector $\sigma \cdot \mathbf{n}$;

$$\sigma \cdot \mathbf{n} = -p\mathbf{n} + \gamma \mathcal{K}\mathbf{n}, \tag{3.1}$$

where $\mathbf{n}$ is the normal to the deformed droplet surface, p the pressure in the droplet and the 'total curvature' $\mathcal{K}$ is the sum of the local principal curvatures. Importantly, the interfacial stress is treated as a constant, isotropic and strain-independent surface tension γ, which is an excellent approximation for a wide range of soft materials (e.g. [12]).

The bulk modulus K^* of the equivalent elastic inclusion can be calculated (e.g. [27]) by considering a spherical particle embedded in an infinite host material subjected to a spherically symmetric strain at infinity, yielding

$$K^* = K_{\text{incl}} + \frac{2\gamma}{3R}, \tag{3.2}$$

where R is the radius of the liquid inclusion, and K_{incl} is the bulk modulus that the inclusion would have in the absence of surface effects. Thus, $K^* \to \infty$ as $K_{\text{incl}} \to \infty$ in our incompressible droplet inclusions.

We obtain the shear modulus μ^* of the equivalent elastic inclusion by comparing Eshelby's results for the elastic moduli of a dilute composite with incompressible spherical elastic inclusions:[1]

$$\bar{K}^{\text{dil}} = \frac{K}{1 - \alpha^{-1}\phi}, \quad \alpha = \frac{1+\nu}{3(1-\nu)} \tag{3.3a}$$

and

$$\bar{\mu}^{\text{dil}} = \frac{\mu}{1 + B\phi}, \quad B = \frac{\mu^* - \mu}{(\mu - \mu^*)\beta - \mu}, \quad \beta = \frac{2}{15}\frac{4-5\nu}{1-\nu} \tag{3.3b}$$

to Style *et al.*'s result for the Young's modulus of a dilute composite containing incompressible liquid droplets [7, eqn (19)]:

$$\frac{\bar{E}^{\text{dil}}}{E} = \left[1 + \frac{3(1-\nu)[(R/L)(1+13\nu) - (9 - 2\nu + 5\nu^2 + 16\nu^3)]}{(1+\nu)[(R/L)(7-5\nu) + (17 - 2\nu - 19\nu^2)]}\phi\right]^{-1}. \tag{3.4}$$

[1]The last two equations in Eshelby [1, p. 390].

Using equation (3.3*a*) and noting $\bar{\mu}^{\mathrm{dil}} = 3\bar{K}^{\mathrm{dil}}\bar{E}^{\mathrm{dil}}/(9\bar{K}^{\mathrm{dil}} - \bar{E}^{\mathrm{dil}})$, equation (3.4) becomes

$$\frac{\bar{\mu}^{\mathrm{dil}}}{\mu} = \frac{17 - 2\nu - 19\nu^2 + (R/L)(7 - 5\nu)}{17 - 2\nu - 19\nu^2 + 15(\nu^2 - 1)\phi + (R/L)(7 - 5\nu - 15(\nu - 1)\phi)}. \tag{3.5}$$

Thus, we equate equations (3.3*b*) and (3.5) to obtain

$$\frac{\mu^*}{\mu} = \frac{8(1+\nu)}{3(1+\nu) + 5(R/L)}. \tag{3.6}$$

This agrees with [18] in the limit of an incompressible matrix. Finally, the equivalent Young's modulus is

$$\frac{E^*}{E} = \frac{3\mu^*}{2\mu(1+\nu)} = \frac{4}{1 + \nu + (5/3)(R/L)}. \tag{3.7}$$

It is important to note that although a finite value of the volume fraction $\phi \ll 1$ is assumed in the derivation of the equivalent moduli in equations (3.2), (3.6) and (3.7), all are *independent of* ϕ. In the case of an incompressible matrix ($\nu = \frac{1}{2}$), we recover the expression for E^* of Style *et al.*, [8, eqn (9)],

$$\left(\frac{E^*}{E}\right) = \frac{24(L/R)}{10 + 9(L/R)}. \tag{3.8}$$

Now, for arbitrary Poisson's ratio ν of the host matrix, we find that (a) when $R \gg L$ the droplets behave like inclusions with Young's modulus $E^* = 12\gamma/5R$, and (b) when $R \ll L$, in the capillarity-dominated regime, the equivalent Young's modulus of each inclusion saturates at $E^* = 4E/(1+\nu)$. This shows that despite the widespread ansatz that $E^* = 2\gamma/R$, the effective stiffness cannot become arbitrarily large as the droplet shrinks. Therefore, the limits (a) and (b) found by Style *et al.* [7] for an incompressible host matrix, $E^* \to 12\gamma/5R$ ($R \gg L$) and $E^* \to 8E/3$ ($R \ll L$), respectively, are consistent with a more general theory.

4. The effective composite moduli

Having obtained equations for the equivalent inclusion moduli, K^*, μ^*, we can substitute them into equations (2.1) and (2.2) to obtain

$$\frac{\bar{K}}{K} = \lim_{K^* \to \infty}\left[1 + \frac{\phi(K^* - K)}{K + (1-\phi)(K^* - K)S_m}\right] = 1 + \frac{\phi}{(1-\phi)S_m} \tag{4.1}$$

and

$$\frac{\bar{\mu}}{\mu} = 1 - \frac{15(\nu - 1)(1 - R/L + \nu)\phi}{(R/L)[7 + 8\phi - 5\nu(1 + 2\phi)] + (1+\nu)[17 - 8\phi + \nu(10\phi - 19)]}. \tag{4.2}$$

Hence from equations (4.1) and (4.2), one finds

$$\frac{\bar{E}}{E} = \frac{(3/2(1+\nu)(1-2\nu))(\bar{K}/K)(\bar{\mu}/\mu)}{(1/(1-2\nu))(\bar{K}/K) + (1/2(1+\nu))(\bar{\mu}/\mu)} = \frac{\nu(4\phi - 1) - (2\phi + 1)}{1+\nu}\frac{f_1 + (R/L)f_2}{f_3 + (R/L)f_4}, \tag{4.3}$$

with

$$\left.\begin{aligned} f_1(\nu,\phi) &= -(1+\nu)[\nu(19 + 5\phi) - (17 + 7\phi)] \\ f_2(\nu,\phi) &= (5\nu - 7)(\phi - 1) \\ f_3(\nu,\phi) &= (1+\nu)(19\nu - 17) + [44\nu - 14 + 2(5 - 24\nu)\nu^2]\phi \\ &\quad + [13 - 15\nu + 2\nu(15\nu - 13) + \nu(2\nu - 1)(-13 + 15\nu)]\phi^2 \\ \text{and} \quad f_4(\nu,\phi) &= 5\nu - 7 + 2(7\nu - 5)\phi + (1 - 2\nu)(15\nu - 13)\phi^2, \end{aligned}\right\} \tag{4.4}$$

and hence as expected in the dilute limit ($\phi \to 0$) of equation (4.3) we recover equation (3.4).

Next we focus on the special case of an incompressible matrix ($\nu = \frac{1}{2}$), where the identity $E_{\mathrm{rel}} \equiv (\bar{E}/E) = (\bar{\mu}/\mu) \equiv \mu_{\mathrm{rel}}$ holds. In some experimental situations, it is interesting to know the effective Young's modulus for an incompressible matrix with a finite concentration of monodisperse

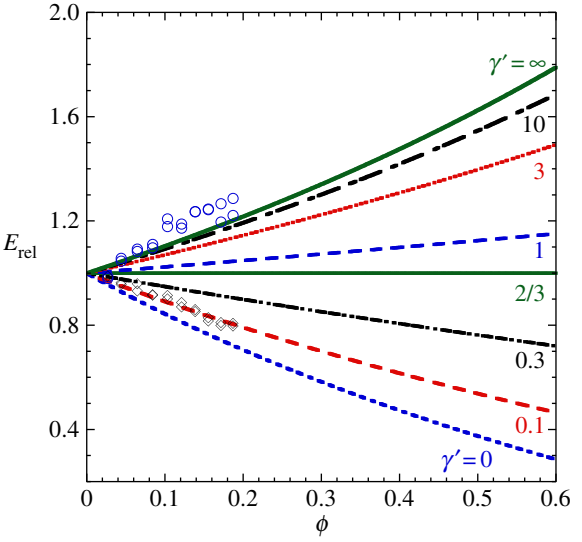

Figure 2. In the incompressible matrix case, E_{rel} versus ϕ for a wide range of γ' from the softening to the stiffening regime, according to the EIAS theory. The experimental data are from Style *et al.* [8]; see their fig. 4*b*. (Online version in colour.)

inclusions of arbitrary size where the bulk elasticity ($R \gg L$) or the capillarity-dominated ($R \ll L$) limits manifest themselves. Here, equation (4.3) takes the simpler form

$$\left(\frac{\bar{E}}{E}\right) = \frac{15 + 9\phi + (R/L)(6 - 6\phi)}{15 - 6\phi + (R/L)(6 + 4\phi)}, \tag{4.5}$$

whose large and small droplet limits are

$$\left(\frac{\bar{E}}{E}\right) = \begin{cases} \dfrac{3 - 3\phi}{3 + 2\phi}, & R \gg L \\ \dfrac{5 + 3\phi}{5 - 2\phi}, & R \ll L. \end{cases} \tag{4.6}$$

When, as above, the elastocapillary length is based on the matrix material, $L \equiv \gamma/E$, a natural dimensionless parameter is $\gamma' \equiv L/R = \gamma/(ER)$, which we use to rewrite equation (4.5) as

$$E_{rel}|_{\nu=1/2} = \frac{2 - 2\phi + \gamma'(5 + 3\phi)}{2 + (4/3)\phi + \gamma'(5 - 2\phi)}. \tag{4.7}$$

Figure 2 shows E_{rel} of equation (4.7) versus ϕ, and in figure 3 it is plotted against $R/[(3V/4\pi)^{1/3}]$, where V is the volume of composite per inclusion. We see in figure 2 that the $\gamma' = L/R < \frac{2}{3}$ ($\gamma' > \frac{2}{3}$) softening (stiffening) behaviour spans the experimental range seen by Style *et al.* [8], and bounds that behaviour in the dilute limit to within experimental error in the same manner as seen in their fig. 4*b*. We also find exact 'mechanical cloaking', where E_{rel} is constant at $\gamma' = \frac{2}{3}$ for all liquid volume fractions. Precisely, the same cloaking condition is found in the dilute theory [7], *and* from a complementary generalized three-phase self-consistent approach [28] (again independent of ϕ).

As γ' becomes arbitrarily large (or the droplets become arbitrarily small), equation (4.6) shows that the capillary-dominated stiffening regime asymptotes to $E_{rel}|_{\nu=1/2} \to (5 + 3\phi)/(5 - 2\phi)$. This is the upper limit of rigidity, scaling as $1/(1 - \phi)$ at small ϕ (figure 2).

Finally, we note that in the limit $\phi \to 0$, the present theory quantitatively captures the dilute theory [7]. In figures 4 and 5, we compare these two predictions of E_{rel} for the incompressible matrix case. Clearly, the EIAS theory is softer than the dilute theory in both the softening ($\gamma' < \frac{2}{3}$)

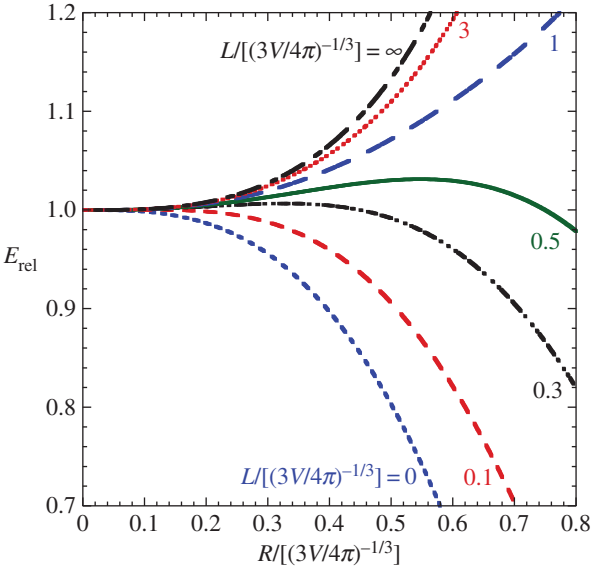

Figure 3. In the incompressible matrix case E_{rel} versus $R/[(3V/4\pi)^{1/3}]$ for a wide range of the parameter $L/[(3V/4\pi)^{1/3}]$, according to the EIAS theory, where $(3V/4\pi)^{1/3}$ represents an average inter-inclusion distance. (Online version in colour.)

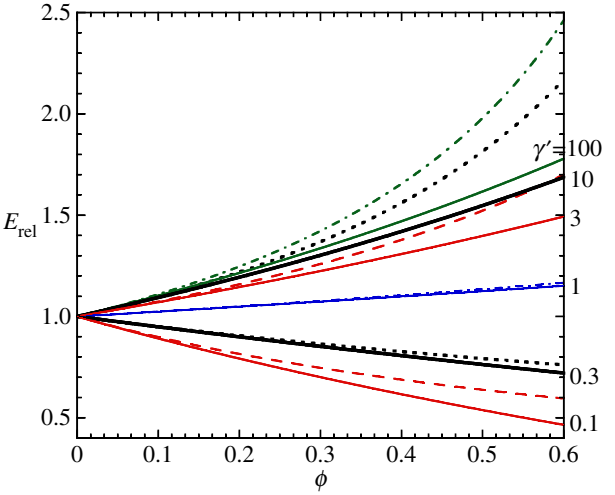

Figure 4. In the incompressible matrix case, E_{rel} versus ϕ for the EIAS (solid curves, equation (4.7)) and dilute (dotted/dashed curves, [7]) theories over a wide range of γ' from the softening to the stiffening regime. From the bottom to the top, the solid EIAS curves correspond to $\gamma' = 0.1, 0.3, 1, 3, 10, 100$. The dilute theory curves correspond to $\gamma' = 0.1$ (red, dashed line), 0.3 (black, dotted line), 1 (blue, dashed-dotted line), 3 (red, dashed line), 10 (black, dotted line) and 100 (green, dashed-dotted line). (Online version in colour.)

and the stiffening ($\gamma' > \frac{2}{3}$) regimes. Importantly, for volume fractions up to $\phi \approx 0.2$ (after which the dilute theory begins to break down), there is only a few per cent deviation, as shown in figure 5. This is well within experimental error [8] and thus we show that the dilute theory provides an accurate and simple framework for comparison, given that it is the appropriate asymptotic limit of the non-dilute theory. It is only when ϕ increases that large deviations appear, and these are most

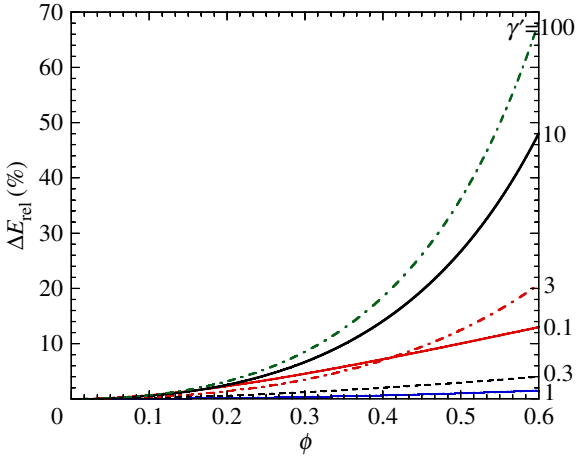

Figure 5. In the incompressible matrix case, the per cent deviation between the dilute and EIAS theories $\Delta E_{\rm rel}$ versus ϕ, shown for the same values of γ' as in figure 4: 0.1 (red, solid line), 0.3 (black, dashed line), 1 (blue, solid line), 3 (red, dashed-dotted line), 10 (black, solid line) and 100 (green, dashed-dotted line). (Online version in colour.)

pronounced for large γ'. Independent of ϕ, the two theories predict precisely the same mechanical cloaking condition of the inclusions; $\gamma' = \frac{2}{3}$.

5. Conclusion

In the light of recent work showing unexpected stiffening behaviour of the effective elastic response of soft materials with liquid inclusions [7,8], we have revisited the Mori–Tanaka, or EIAS, method for composite materials to account for the (strain-independent) liquid/matrix interfacial tension. The motivation is that while Style *et al.* [7,8] explained experimental data using a dilute theory, we sought to understand the limits of the dilute approximation by extending a known approach for non-dilute systems to account for the stiffening behaviour associated with interfacial forces. In so doing, we quantitatively analysed when the dilute theory breaks down and thus confirmed that the comparison of experiment and theory [8] occurred in the regime where the dilute theory is valid.

In detail, we extended the EIAS theoretical framework for the elastic moduli of composites, by taking into account the surface tension at the droplet/host-matrix interface when the matrix is a linear-elastic material. The dilute limit of the EIAS theory is achieved by taking $\phi \to 0$, and we find that the effective Young's modulus depends solely on two parameters; ϕ and $\gamma' = L/R$. We have examined this graphically in the incompressible case of $\nu = \frac{1}{2}$. These models, along with a generalized self-consistent three-phase theory [28], predict the same exact cloaking condition of the far-field signatures associated with the presence of the inclusions, *viz.*, $R = 3L/2$, independent of volume fraction ϕ.

There are a range of possible comparisons and tests that immediately come to mind. For example, in situations wherein the host matrix is a nonlinear elastic (e.g. [29,30]) or viscoelastic (e.g. [16]) material. Finally, it would be of interest to compare this framework and that in our companion paper [28], in which we treat the inclusion/matrix interface using a strain-independent surface tension within the framework of an interfacial stress model (e.g. [31,32]). In [28], we noted that there is a similarity between this class of problems and a saturated poroelastic system (e.g. [33–37], for both overviews and recent results), where the deformation of the host material is controlled by the value of ϕ. We suggested that these effective medium theories may be of use in attempting to constrain the ϕ-dependence of transport properties in poroelastic systems, such as the flow permeability.

Ethics. The research in this paper presented no ethical concerns.
Data accessibility. This paper has no data.
Authors' contributions. J.S.W. and R.W.S. conceived of and designed the study. F.M., R.W.S. and J.S.W. carried out the analysis and drafted the manuscript. All authors gave final approval for publication
Competing interests. We have no competing interests.
Funding. F.M. and J.S.W. acknowledge Swedish Research Council grant no. 638-2013-9243 and the 2015 Geophysical Fluid Dynamics Summer Study Program at the Woods Hole Oceanographic Institution, which is supported by the National Science Foundation and the Office of Naval Research under OCE-1332750. J.S.W. also acknowledges a Royal Society Wolfson Research Merit Award.
Acknowledgements. The authors thank Eric Dufresne and Dhruba Mitra for helpful comments and encouragement.

References

1. Eshelby JD. 1957 The determination of the elastic field of an ellipsoidal inclusion, and related problems. *Proc. R. Soc. Lond. A* **241**, 376–396. (doi:10.1098/rspa.1957.0133)
2. Hashin Z, Shtrikman S. 1963 A variational approach to the theory of the elastic behaviour of multiphase materials. *J. Mech. Phys. Solids* **11**, 127–140. (doi:10.1016/0022-5096(63)90060-7)
3. Hashin Z. 1962 The elastic moduli of heterogeneous materials. *J. Appl. Mech., Trans. ASME* **29**, 143–150. (doi:10.1115/1.3636446)
4. Christensen RM, Lo KH. 1979 Solutions for effective shear properties in three phase sphere and cylinder models. *J. Mech. Phys. Solids* **27**, 315–330. (doi:10.1016/0022-5096(79)90032-2)
5. Cauvin L, Bhatnagar N, Brieu M, Kondo D. 2007 Experimental study and micromechanical modeling of MMT platelet-reinforced PP nanocomposites. *C. R. Mech.* **335**, 702–707. (doi:10.1016/j.crme.2007.07.007)
6. Fornes T, Paul D. 2003 Modeling properties of nylon 6/clay nanocomposites using composite theories. *Polymer* **44**, 4993–5013. (doi:10.1016/S0032-3861(03)00471-3)
7. Style RW, Wettlaufer JS, Dufresne ER. 2015 Surface tension and the mechanics of liquid inclusions in compliant solids. *Soft Matter* **11**, 672–679. (doi:10.1039/C4SM02413C)
8. Style RW, Boltyanskiy R, Allen B, Jensen KE, Foote HP, Wettlaufer JS, Dufresne ER. 2015 Stiffening solids with liquid inclusions. *Nat. Phys.* **11**, 82–87. (doi:10.1038/nphys3181)
9. Mori T, Tanaka K. 1973 Average stress in matrix and average elastic energy of materials with misfitting inclusions. *Acta Metall.* **21**, 571–574. (doi:10.1016/0001-6160(73)90064-3)
10. Christensen RM. 2012 *Mechanics of composite materials*. New York, NY: Dover.
11. Cahn JW. 1978 Thermodynamics of solid and fluid surfaces. In *Segregation to interfaces* (eds JJ Blakely, WC Johnson) ASM Seminar Series, pp. 3–23. Cleveland, OH: ASM Press.
12. Hui C-Y, Jagota A. 2013 Surface tension, surface energy, and chemical potential due to their difference. *Langmuir* **29**, 11 310–11 316. (doi:10.1021/la400937r)
13. Style RW, Boltyanskiy R, Che Y, Wettlaufer JS, Wilen LA, Dufresne ER. 2013 Universal deformation of soft substrates near a contact line and the direct measurement of solid surface stresses. *Phys. Rev. Lett.* **110**, 066103. (doi:10.1103/PhysRevLett.110.066103)
14. Mora S, Maurini C, Phou T, Fromental J-M, Audoly B, Pomeau Y. 2013 Solid drops: large capillary deformations of immersed elastic rods. *Phys. Rev. Lett.* **111**, 114301. (doi:10.1103/PhysRevLett.111.114301)
15. Naderman N, Hui C-Y, Jagota A. 2013 Solid surface tension measured by a liquid drop under a solid film. *Proc. Natl Acad. Sci. USA* **110**, 10 541–10 545. (doi:10.1073/pnas.1304587110)
16. Palierne J. 1990 Linear rheology of viscoelastic emulsions with interfacial tension. *Rheol. Acta* **29**, 204–214. (doi:10.1007/BF01331356)
17. Thy Linh N-T, Ducloue L, Ovarlez G, Chateau X. 2013 Overall properties of a soft porous material: surface tension effects. In *Poromechanics V: Proc. of the Fifth Biot Conf. on Poromechanics, 10–12 July, Vienna, Austria* (eds C Hellmich, B Pichler, D Adam), pp. 1895–1902. Reston, VA: ASCE. (doi:10.1061/9780784412992.224)
18. Ducloue L, Pitois O, Goyon J, Chateau X, Ovarlez G. 2014 Coupling of elasticity to capillarity in soft aerated materials. *Soft Matter* **10**, 5093–5098. (doi:10.1039/c4sm00200h)
19. Sharma P, Ganti S. 2004 Size-dependent Eshelby's tensor for embedded nano-inclusions incorporating surface/interface energies. *J. Appl. Mech.* **71**, 663–671. (doi:10.1115/1.1781177)
20. Duan HL, Wang J, Huang ZP, Karihaloo BL. 2005 Size-dependent effective elastic constants of solids containing nano-inhomogeneities with interface stress. *J. Mech. Phys. Solids* **53**, 1574–1596. (doi:10.1016/j.jmps.2005.02.009)

21. Le Quang H, He Q-C. 2007 Size-dependent effective thermoelastic properties of nanocomposites with spherically anisotropic phases. *J. Mech. Phys. Solids* **55**, 1899–1931. (doi:10.1016/j.jmps.2007.02.005)
22. Le Quang H, He Q-C. 2008 Variational principles and bounds for elastic inhomogeneous materials with coherent imperfect interfaces. *Mech. Mater.* **40**, 865–884. (doi:10.1016/j.mechmat.2008.04.003)
23. Brisard S, Dormieux L, Kondo D. 2010 Hashin–Shtrikman bounds on the shear modulus of a nanocomposite with spherical inclusions and interface effects. *Comput. Mater. Sci.* **50**, 403–410. (doi:10.1016/j.commatsci.2010.08.032)
24. Brisard S, Dormieux L, Kondo D. 2010 Hashin–Shtrikman bounds on the bulk modulus of a nanocomposite with spherical inclusions and interface effects. *Comput. Mater. Sci.* **48**, 589–596. (doi:10.1016/j.commatsci.2010.02.027)
25. Benveniste Y. 1987 A new approach to the application of Mori–Tanaka's theory in composite materials. *Mech. Mater.* **6**, 147–157. (doi:10.1016/0167-6636(87)90005-6)
26. Wu TT. 1966 The effect of inclusion shape on the elastic moduli of a two-phase material. *Int. J. Solids Struct.* **2**, 1–8. (doi:10.1016/0020-7683(66)90002-3)
27. Huang Z, Wang J. 2013 Micromechanics of nanocomposites with interface energy effect. In *Handbook of micromechanics and nanomechanics* (eds S Li, X-L Gao), ch. 8. Pan Stanford Publishing.
28. Mancarella F, Style RW, Wettlaufer JS. 2016 Interfacial tension and a generalized three-phase self-consistent theory of soft composite solids in the non-dilute regime. *Soft Matter* **12**, 2744–2750. (doi:10.1039/c5sm03029c)
29. Ponte Castanẽda P, Suquet P. 1997 Nonlinear composites. *Adv. Appl. Mech.* **34**, 171–302. (doi:10.1016/S0065-2156(08)70321-1)
30. Jiang B, Weng GJ. 2004 A generalized self-consistent polycrystal model for the yield strength of nanocrystalline materials. *J. Mech. Phys. Solids* **52**, 1125–1149. (doi:10.1016/j.jmps.2003.09.002)
31. Duan HL, Wang J, Huang ZP, Karihaloo BL. 2005 Eshelby formalism for nano-inhomogeneities. *Proc. R. Soc. A* **461**, 3335–3353. (doi:10.1098/rspa.2005.1520)
32. Duan HL, Yi X, Huang ZP, Wang J. 2007 A unified scheme for prediction of effective moduli of multiphase composites with interface effects. Part I: theoretical framework. *Mech. Mater.* **39**, 81–93. (doi:10.1016/j.mechmat.2006.02.009)
33. Coussy O. 2004 *Poromechanics*. New York, NY: Wiley.
34. Wang HF. 2000 *Theory of linear poroelasticity*. Princeton, NJ: Princeton University Press.
35. MacMinn CW, Dufresne ER, Wettlaufer JS. 2015 Fluid-driven deformation of a soft granular material. *Phys. Rev. X* **5**, 011020. (doi:10.1103/PhysRevX.5.011020)
36. Hewitt DR, Nijjer JS, Worster MG, Neufeld JA. 2016 Flow-induced compaction of a deformable porous medium. *Phys. Rev. E* **93**, 023116. (doi:10.1103/PhysRevE.93.023116)
37. MacMinn CW, Dufresne ER, Wettlaufer JS. 2016 Large deformatons of a soft porous material. *Phys. Rev. Applied* **5**, 044020. (doi:10.1103/PhysRevApplied.5.044020)